



1 **Performance evaluation of multiple satellite rainfall products for Dhidhessa River Basin**
2 **(DRB), Ethiopia**

3 **Gizachew Kabite Wedajo^{a,b*}, Misgana Kebede Muleta^c, Berhan Gessesse Awoke^{b,d}**

4 ^aDepartment of Earth Sciences, Wollega University, P.O.Box 395, Nekemte, Ethiopia

5 ^bDepartment of Remote Sensing, Entoto Observatory Research Center, Ethiopia Space Science
6 Technology Institute, P.O.Box 33679, Addis Ababa, Ethiopia

7 ^cDepartment of Civil and Environmental Engineering, California Polytechnic State University,
8 San Luis Obispo, California, 93407

9 ^dDepartment of Geography and Environmental Studies, Kotebe Metropolitan University, Addis
10 Ababa, Ethiopia

11 *Correspondence: Email: Kabiteg@gmail.com; Mobile: [0911951952](tel:0911951952)

12



13 **Abstract**

14 *Precipitation is a crucial driver of hydrological processes. Ironically, reliable characterization*
15 *of its spatiotemporal variability is challenging. Ground-based rainfall measurement using rain*
16 *gauges can be more accurate. However, installing a dense gauging network to capture rainfall*
17 *variability can be impractical. Satellite-based rainfall estimates (SREs) can be good*
18 *alternatives, especially for data-scarce basins like in Ethiopia. However, SREs rainfall is*
19 *plagued with uncertainties arising from many sources. The objective of this study was to*
20 *evaluate the performance of the latest versions of several SREs products (i.e., CHIRPS2,*
21 *IMERG6, TAMSAT3 and 3B42/3) for the Dhidhessa River Basin (DRB). Both statistical and*
22 *hydrologic modelling approaches were used for the performance evaluation. The Soil and*
23 *Water Analysis Tool (SWAT) was used for hydrological simulations. The results showed that*
24 *whereas all four SREs products are promising to estimate and detect rainfall for the DRB, the*
25 *CHIRPS2 dataset performed the best at annual, seasonal and monthly timescales. The*
26 *hydrologic simulation based evaluation showed that SWAT's calibration results are sensitive*
27 *to the rainfall dataset. The hydrologic response of the basin is found to be dominated by the*
28 *subsurface processes, primarily by the groundwater flux. Overall, the study showed that both*
29 *CHIRPS2 and IMERG6 products can be reliable rainfall data sources for hydrologic analysis*
30 *of the Dhidhessa River Basin.*

31 **Keywords:** *Satellite-based rainfall estimates; Dhidhessa River Basin; Performance evaluation;*
32 *Statistical evaluation; Hydrological modelling performance.*

33



34 1. Introduction

35 Precipitation is an important hydrological component (Behrangi et al., 2011; Meng et
36 al., 2014). Accurate representation of its spatiotemporal variability is crucial to improves
37 hydrological modelling (Grusson et al., 2017). Ironically, precipitation is one of the most
38 challenging hydrometeorological data to be accurately represented (Yong et al., 2014).
39 Climatic and topographic conditions are the primary factors that affect the accuracy of rainfall
40 measurements.

41 Rainfall is measured either using ground-based (i.e., rain gauge and radar) or satellite
42 sensors, where all measurement methods exhibit limitations (Thiemig et al., 2013). Ground-
43 based rainfall measurements are direct and generally accurate near the sensor location.
44 However, they are either of poor density to represent spatial and temporal variability of
45 precipitation, or may not even exist (e.g., radars), especially in developing countries (Behrangi
46 et al., 2011). Ground-based rainfall measurement techniques provide point and incomplete
47 measurements (Kidd et al., 2012; Maggioni et al., 2016). It may also be infeasible to install and
48 maintain dense ground-based gauging stations in remote areas like mountains, deserts, forests
49 and large water bodies (Dinku et al., 2018; Tapiador et al., 2012). However, satellite-based
50 rainfall estimates (SREs) provide high-resolution precipitation data including in areas where
51 ground-based rainfall measurements are impractical, sparse, or non-existent (Stisen and
52 Sandholt, 2010).

53 Consequently, high-resolution precipitation products have been developed over the last
54 three decades. These products include Tropical Rainfall Measuring Mission (TRMM) Multi-
55 satellite Precipitation Analysis (TMPA; Huffman et al., 2007), the Precipitation Estimation
56 from Remote Sensing Information Using Artificial Neuron Networks (PERSIANN;
57 Sorooshian et al., 2000), Climate Prediction Center (CPC) morphing algorithm (CMORPH)
58 (Joyce et al., 2004), African Rainfall Climatology (ARC) (Xie and Arkin 1995), Tropical
59 Applications of Meteorology using SATellite (TAMSAT) (Maidment et al., 2017) and the
60 Climate Hazards Group Infrared Precipitation with Stations (CHIRPS) (Funk et al., 2015).
61 The consistency, spatial coverage, accuracy and spatiotemporal resolution of SREs have
62 improved overtime (Behrangi et al., 2011).

63 As indirect rainfall estimation techniques, SREs products possess uncertainties
64 resulting from errors in measurement, sampling, retrieval algorithm, and bias correction



65 processes (Dinku et al., 2010; Gebremichael et al., 2014; Tong et al., 2014). Local topography
66 and climatic conditions can also affect the accuracy of SREs estimation (Bitew and
67 Gebremichael, 2011). Hence, SREs products should be carefully evaluated before using the
68 products for any application. Statistical and hydrological modelling are two common methods
69 for evaluating SREs. The statistical evaluation method examines the intrinsic precipitation data
70 quality including its spatiotemporal characteristics via pairwise comparison of the SREs
71 products and ground observations. Scale mismatches between SREs products and ground-
72 based measurements is a typical drawback. The hydrological modelling method evaluates the
73 performance of a SREs product for a specific application such as streamflow predictive ability
74 at watershed scale (Su et al., 2017). The two methods complement each other where the
75 statistical method provides information on data quality while the hydrological model technique
76 assesses the usefulness of the data for hydrological applications (Thiemig et al., 2013).
77 However, most studies used only statistical evaluation methods (e.g., Dinku et al., 2018; Ayehu
78 et al., 2018).

79 Studies have recommended SREs products for data scarce basins (Behrangi et al., 2011;
80 Bitew and Gebremichael, 2011; Thiemig et al., 2013). However, there is no consensus
81 regarding “best” SREs product for different climatic regions. Nesbitt et al. (2008) found that
82 CMORPH and PERSIANN produced higher rainfall rates compared to TRMM for the
83 mountain ranges of Mexico. Dinku et al. (2008) reported better performance of the TRMM and
84 CMORPH products in Ethiopia and Zimbabwe whereas PERSSINN outperformed TRMM in
85 South America according to de Goncalves et al. (2006). Interestingly, the performance of SREs
86 products seems to differ even within a basin. For the Blue Nile basin in Ethiopia, for example,
87 CMORPH overestimated precipitation for the lowland areas but underestimated for the
88 highlands (Bitew and Gebremichael, 2011; Habib et al., 2012; Gebremichael et al., 2014). The
89 discrepancy in the findings of these studies shows the performance of SREs varies with region,
90 topography, season, and climatic conditions of the study area (Kidd and Huffman, 2011;
91 Seyyedi et al., 2015; Nguyen et al., 2018; Dinku et al., 2018). As such, many studies have
92 recommended SREs evaluation at a local scale to verify its performance for specific
93 applications (Hu et al., 2014; Toté et al., 2015; Kimani et al., 2017; Ayehu et al., 2018).

94 Studies have examined the performance of SREs in Ethiopia (Haile et al., 2013;
95 Worqlul et al., 2014; Ayehu et al., 2018; Dinku et al., 2018). However, majority of these studies
96 used the statistical method to evaluate SREs, and no study has been completed for the



97 Dhidhessa River Basin (DRB). With only 0.32 rain gauges per 1000 km², the DRB meets the
98 World Meteorological Organization (WMO) data-scarce basin classification (WMO, 1994).
99 The objective of this study was to evaluate the performance of various SREs products in terms
100 of characterizing the spatiotemporal distribution of rainfall in the DRB. The study could assist
101 with the planning and management of existing and planned water resources projects in the
102 basin.

103 SREs are continuously updated to minimize bias and uncertainty. Evaluating and
104 validating improved products for various climatic regions would be valuable (Kimani et al.,
105 2017). Recently improved SREs products include Tropical Rainfall Measuring Mission
106 (TRMM) Multi-Satellite Precipitation Analysis version 7 (here after referred to as 3B43 for
107 monthly and 3B42 for daily products), Climate Hazards Group Infrared Precipitation with
108 Stations version 2 (CHIRPS2), Tropical Applications of Meteorology using SATellite version
109 3 (TAMSAT3) and Integrated Multi-satellitE Retrievals for GPM version 6B (IMERG6).
110 Studies have reported improvements of these new versions compared to their predecessors.
111 However, to the best of our knowledge, the rainfall detection and hydrological simulation
112 capability of these SREs datasets were not evaluated for the basins in Ethiopian including the
113 DRB. This study examined the latest SREs products in terms of their rainfall detection and
114 estimation skills, and improving hydrological prediction for DRB, a medium-sized river basin
115 with scarce gauging data. As such, the objectives of this study were: 1) to evaluate the intrinsic
116 rainfall data quality and detection skills of multiple SREs products (i.e., 3B42/3, CHIRPS2,
117 TAMSAT3, and IMERG6), and 2) to examine hydrologic prediction performances of SREs for
118 the DRB. The Soil and Water Assessment Tool (SWAT), a physically based distributed model
119 that has performed well in humid tropical regions like Ethiopia, was used for the hydrologic
120 simulation.

121 **2. Methods and Materials**

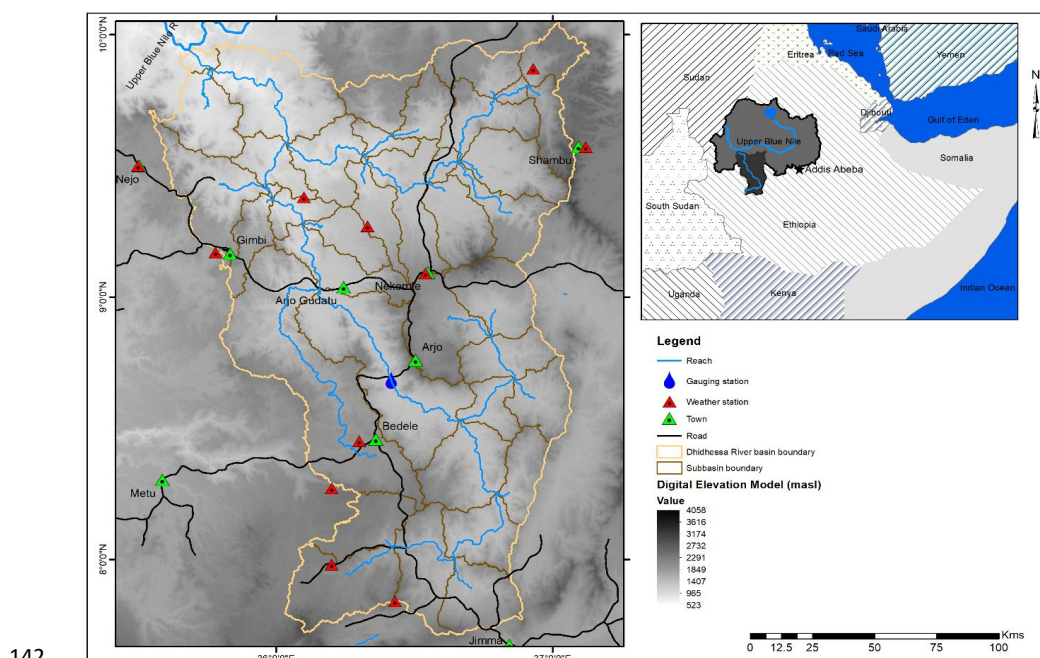
122 **2.1. Descriptions of the study area**

123 The Dhidhessa River drains to the Blue Nile River (Figure 1). It is one of the largest
124 and most important River basins in Ethiopia in terms of its physiography and hydrology
125 (Yohannes, 2008). Located between 7°42'43"N to 10°2'55"N latitude and 35°31'23"E to
126 37°7'60"E longitude, the River basin exhibits highly variable topography that ranges from 619
127 m to 3213 m above mean sea level (a.m.s.l). The Dhidhessa River starts from the Sigo



128 mountain ranges and travels 494 km before it joins the Blue Nile River around the Wanbara
129 and Yaso districts. The outlet considered for this study is the confluence of the Dhidhessa River
130 and the Blue Nile River which covers a total drainage area of 28,175 km². The River basin has
131 many perennial tributaries (Figure 1).

132 Temperature and precipitation in the Dhidhessa River basin exhibit substantial spatial
133 and seasonal variability. The mean maximum and minimum daily air temperatures in the River
134 basin range from 20-33 °C and 6-19 °C, respectively. The long-term mean annual rainfall ranges
135 from 1200 mm to 2200 mm in the River basin. Soils in the River basin are generally deep and
136 have high organic content implying they have high infiltration potential. The dominant soil
137 type is Acrisols while Cambisols and Nitisols are common (OWWDSE, 2014). Igneous,
138 sedimentary and metamorphic rocks are but igneous rock, particularly basalt, is dominant in
139 the basin (GSE, 2000). Forest, shrubland, grassland, and agriculture are the dominant land
140 cover types in the basin (Kabite et al., 2020). Major crops include perennial and cash crops like
141 coffee, Mango, and Avocado (OWWDSE, 2014).



142
143 Figure 1. Location map of Dhidhessa River basin with ground stations (USGS, 1998).

144



145 **2.2. Data sources and descriptions**

146 For this study, we used different spatial and temporal datasets such as Digital Elevation
147 Model (DEM), climate, streamflow, soil and land cover from different sources (Table 1).

148 Table 1. Data description and sources.

Data type	Data acquisition	Resolution	Sources
SRTM DEM	1998	30 * 30 m	USGS
3B42/3	1998-recent present	0.25° (~25 km)	NASA & JAXA
CHIRPS2	1980-present	0.05° (~5 km)	USGS & Climate Hazard Group
TAMSAT3	1980-present	0.0375° (~4 km)	Reading University
IMERG6	2001-present	0.1° (~10 km)	NASA & JAXA
Streamflow data	1980-2014	Daily	EMoWI
Meteorological data	1980-014	Daily	NMA
Land cover	2001	30*30 m	Kabite et al. (2020)
Soil map	2013/14	variable	EMoWI, FAO & OWWDSE

149 Shuttle Radar Thematic Mapper (SRTM) derived Digital Elevation Model (DEM) of
150 30*30 m spatial resolution was obtained from the United States Geological Survey (USGS). It
151 is one of the input data for SWAT model from which topographic and drainage parameters
152 (e.g., drainage pattern, slope and watershed boundary) were derived. Soil map of 1:250,000
153 scale were obtained from source described in Table 1. Soil physical properties required for
154 SWAT model were derived from the soil map. Supervised image classification was used to
155 prepare land cover map of 2001. Together with land cover and soil maps, DEM was used to
156 create Hydrologic Response Units (HRUs).

157 Rainfall data for nine stations within the River basin and for three nearby stations
158 (Figure 1), from 2001 to 2014 were obtained from the National Meteorological Agency (NMA)
159 of Ethiopia. The rainfall data was used to evaluate the SREs using the statistical and
160 hydrological modelling evaluation methods. In addition, Enhanced National Climate Time-
161 series Service (ENACTS) gridded (4 m *4 m) minimum and maximum air temperature data
162 was obtained from the National Meteorological Agency (NMA) of Ethiopia. Daily streamflow
163 data from 2001 to 2014 was obtained for a station near the town of Arjo (Figure 1) from
164 Ethiopian Ministry of Water, Irrigation and Energy (EMoWI).



165 The hydrometeorological stations used for this study were selected due to their long-
166 term records and better data quality. The observed streamflow was used to calibrate and
167 validate SWAT model. Land use map for 2001 and soil map were obtained from Kabite et al.
168 (2020) and Ethiopian Ministry of Water, Irrigation and Energy (EMoWI), respectively.

169 2.2.1. Satellite rainfall products

170 The Satellite Rainfall Estimates (SREs) considered in this study include 3B42/3,
171 TAMSAT3, CHIRPS2 and IMERG6. These datasets were selected because of several reasons
172 including that they: i) have relatively high spatial resolution, ii) are gauge-adjusted products,
173 iii) are the latest products and have been found to perform well by recent studies, and iv) were
174 not compared for the basins in Ethiopia particularly IMERG6.

175 The TMPA provides rainfall products for area covering 50°N-50°S for the period of
176 1998 to present at 0.25°*0.25° and 3h spatial and temporal resolution, respectively. The 3h
177 rainfall product is aggregated to daily (3B42) and monthly (3B43) gauge-adjusted post real
178 time precipitation. The performance of the 3B42v7 is superior compared to its predecessor (i.e.,
179 3B42v6) and the real time TMPA product (3B42RT) (Yong et al., 2014). The 3B43 was used
180 in this study for the statistical evaluation while the 3B42 was used for the hydrological
181 performance evaluation. The detail description is given by Huffman et al. (2007).

182 TAMSAT3 algorithm estimates precipitation in an indirect method using cloud-index
183 method, which compares the cold cloud duration (CCD) with predetermined temperature
184 threshold. The CCD is the length of time that a satellite pixel is colder than a given temperature
185 threshold. The algorithm calibrates the CCD using parameters that vary seasonally and spatially
186 but constant from year to year. This makes interannual variations in rainfall to depend only on
187 the satellite observation. The dataset covers the whole Africa at ~4 km and 5-day (pentadal)
188 resolutions for the period of 1983 to present. The original 5-day temporal resolution is
189 disaggregated to daily time-step using daily CCD from which monthly data are derived.
190 TAMSAT3 algorithm are improved compared to its processor (i.e., TAMSAT2). The detail is
191 described in Maidment et al. (2017).

192 The Climate Hazards Group InfraRed Precipitation with Stations (CHIRPS) is a quasi-
193 global precipitation product with ~5km (0.05°) spatial resolution and is available at daily,
194 pentadal (5-day) and monthly timescales. The CHIRPS precipitation data is available from



195 1981 to present. It is gauge-adjusted dataset, which is calculated using weighted bias ratios
196 rather than using absolute station values, which minimizes the heterogeneity of the dataset
197 (Dinku et al., 2018). The latest version of CHIRPS that uses more station data (i.e., CHIRPS
198 version 2) was used in this study. Detail description of CHIRIPS2 is given in Funk et al. (2015).

199 The Global Precipitation Measurement (GPM) is the successor of TMPA with better
200 rainfall detection capability. GPM provides precipitation measurements at 0.1° and half-hourly
201 spatial and temporal resolution. Integrated Multi-satellitE Retrievals for GPM (IMERG) is one
202 of the GPM estimated from all constellation microwave sensors, IR-based observations from
203 geosynchronous satellites, and monthly gauge precipitation data. The IMERG products
204 includes Early Run (near real-time with a latency of 6h), Late Run (reprocessed near real-time
205 with a latency of 18 h) and Final Run (gauge-adjusted with a latency of four months). The
206 IMERG Final Run product provides more accurate precipitation information compared to the
207 near-real time products as it is gauge-adjusted. The latest release of GPM IMERG Final Run
208 version 6B (IMERG6) was used for this study. The detail is given by Huffman et al. (2014).

209 In this study, the performances of 3B42/3, TAMSAT3, CHIRPS2 and IMERG6 rainfall
210 products were evaluated statistically and hydrologically. All the SREs considered in this study
211 are gauge-corrected, and thus bias correction may not be required. Thus, rain gauge stations
212 that were used for validating any of the SREs datasets were excluded for fair comparison. Table
213 1 summarizes details of the data types used for this study.

214 **2.3. Methodology**

215 Satellite rainfall estimates offer several advantages compared to the conventional
216 methods but can also be prone to multiple errors. Rainfall detection capability of the products
217 can be affected by local climate and topography (Xue et al., 2013; Meng et al., 2014).
218 Therefore, performance of SREs should be examined for a particular area before using the
219 products for any application (Hu et al., 2014; Toté et al., 2015; Kimani et al., 2017).

220 The two common SREs performance evaluation methods are statistical (i.e., ground-
221 truthing) and hydrological modelling performance (Behrangi et al., 2011; Bitew and
222 Gebremichael, 2011; Thiemig et al., 2013, Abera et al., 2016; Jiang et al., 2017), and were used
223 in this study. The methods complement each other and their combined application is
224 recommended for more reliable SREs evaluation. The statistical evaluation method involves



225 pairwise comparison of SREs and the rain gauge and/or radar precipitation products. The
226 method provides insight into the intrinsic data quality whereas the modelling approach assesses
227 the usefulness of the data for a desired application (Thiemig et al., 2013). Statistical evaluation
228 was performed for all the SREs products considered in this study (i.e., 3B43, CHIRPS2,
229 TAMSAT3 and IMERG6) to examine their rainfall detection skills. Numerical and categorical
230 validation indices were used to evaluate performance of the products. In addition, the SREs
231 product and gauge datasets were independently used as forcing to calibrate and verify SWAT
232 model. Accordingly, hydrological prediction performance of the rainfall products was
233 evaluated graphically and using statistical indices.

234 **2.3.1. Statistical evaluation of satellite rainfall estimates**

235 Statistical SREs evaluation method was conducted at monthly, seasonal and annual
236 timescales for the overlapping period of all the rainfall data sources (i.e., 2001-2014). A daily
237 comparison was excluded from this study due to weak performance reported in previous studies
238 (Ayehu et al., 2018; Zhao et al., 2017; Li et al., 2018). This is attributed to the measurement
239 time mismatch between ground and satellite rainfall products.

240 Two approaches are commonly used for the statistical evaluation method. The first
241 approach is pixel-to-pixel pair-wise comparisons of the spatially interpolated gauge-based and
242 satellite-based data. The second approach is point-to-pixel pair-wise comparison where
243 satellite rainfall estimates are extracted for each gauge location and the satellite-gauge data
244 pairs are generated and compared. The second approach was used for this study. This is because
245 the 12 rainfall stations considered in this study are unevenly distributed through the basin to
246 accurately represent spatial variability of rainfall in the DRB as required for the first approach.
247 As a result, we chose to extract gauge-satellite rainfall pair values at each rain gauge location
248 instead of interpolating the gauge measurements into gridded products.

249 Accordingly, 168 and 2016 pair data points were extracted for annual and monthly
250 analysis, respectively, and were evaluated using numerical validation indices such as Pearson
251 correlation coefficient (r), bias ratio ($BIAS$), Nash-Sutcliffe efficiency (E) and Root Mean
252 Square Error ($RMSE$). The Pearson correlation coefficient (r) evaluates how well the estimates
253 correspond to the observed values; $BIAS$ reflects how the satellite rainfall estimate over- or
254 under-estimate the rain gauge observations; E shows how well the estimate predicted the



255 observed time series. On the other hand, *RMSE* measures the average magnitude of the estimate
 256 errors. The summary of performance indices are presented in Table 2.

257 Table 2. SREs evaluation indices, mathematical descriptions and perfect score.

Indices	Mathematical expression	Description	Perfect score
Pearson correlation	$r = \frac{\sum(R_g - \bar{R}_g)(R_s - \bar{R}_s)}{\sqrt{\sum(R_g - \bar{R}_g)^2} \sqrt{\sum(R_s - \bar{R}_s)^2}}$	R_g is gauge rainfall observation; R_s satellite rainfall estimates; \bar{R}_g is average gauge rainfall observation; \bar{R}_s is average satellite rainfall estimates	1
Root mean square error (mm)	$RMSE = \sqrt{\frac{\sum(R_g - R_s)^2}{n}}$	n is the number of data pairs; the value ranges from 0 to ∞	0
Bias ratio (BIAS)	$BIAS = \frac{\sum R_s}{\sum R_g}$	A value above (below) 1 indicates an aggregate satellite overestimation (underestimation) of the ground precipitation amounts.	1
Relative bias (RB)	$RB = \frac{\sum(R_s - R_g)}{\sum R_g} * 100$	Describes the systematic bias of the SREs; positive values indicate overestimation while negative values indicate underestimation of precipitation amounts.	0
Mean Error (ME)	$ME = \frac{1}{n} \sum_{i=1}^n (R_s - R_g)$	Describes the average errors of the SREs relative to the observed rainfall data.	0
Nash-Sutcliffe of efficiency coefficient (E)	$E = 1 - \frac{\sum(R_s - R_g)^2}{\sum(R_g - \bar{R}_g)^2}$	The value ranges from $-\infty$ to 1; $0 < E \leq 1$ acceptable while $E \leq 0$ is unacceptable	1
Probability of Detection	$POD = H / (H + M)$	H is the number of hits; M is the number of miss	1
False alarm ratio	$FAR = F / (H + F)$	F is the number of false alarms	0
Critical success index	$CSI = H / (H + M + F)$	Describe the overall skill of the satellite products relative to gauge observation.	1
Percent bias (%)	$PBIAS = \frac{\sum(Q_o - Q_s)}{\sum(Q_o)} * 100$	Q_o is observed discharge; Q_s is simulated discharge for the available pairs of data where $< \pm 15\%$ is very good	0
Coefficient of determination (r^2)	$R^2 = \frac{\sum_{i=1}^n (O_i - \bar{O})(S_i - \bar{S})}{\sqrt{\sum_{i=1}^n (O_i - \bar{O})^2} \sqrt{\sum_{i=1}^n (S_i - \bar{S})^2}}$	O_i & \bar{O} is observed & average streamflow, respectively; S_i & \bar{S} is simulated and average, respectively.	1
Nash-Sutcliffe of coefficient of efficiency	$NSE = \frac{\sum(Q_o - \bar{Q}_o)^2 - \sum(Q_o - Q_s)^2}{\sum(Q_o - \bar{Q}_o)^2}$	\bar{Q}_o is mean value of the observed discharge for the entire time under consideration	1



258 In addition, categorical validation indices such as probability of detection (*POD*), false
259 alarm ratio (*FAR*) and critical success index (*CSI*) were also used for this study. The *POD* score
260 represents the fraction of gauge observations detected correctly by the satellite while the *FAR*
261 shows portion of events identified by the satellite but not confirmed by gauge observations.
262 The *CSI* combines different aspects of the *POD* and *FAR*, describing the overall skill of the
263 satellite products in estimating rainfall.

264 In general, SREs with $r > 0.7$ and relative bias (*RB*) within 10% can be considered as
265 reliable precipitation measurement sources (Brown, 2006; Condom et al., 2011). However,
266 attention should be given to certain indices depending on the application of the product (Toté
267 et al., 2015). For flood forecasting purpose, for example, underestimation of rainfall should be
268 avoided (i.e., mean error (*ME*) > 0 and high *POD* are desirable). In contrast, for drought
269 monitoring, overestimation must be avoided (i.e., *ME* < 0 and low *FAR* is preferred) (Dembélé
270 and Zwart, 2016).

271 **2.3.2. SWAT model setup**

272 Soil and Water Assessment Tool (SWAT) is a semi-distributed, deterministic and
273 continuous simulation watershed model that simulates many water quality and quality fluxes
274 (Arnold et al., 2012). It is a physically based and computationally efficient model that has been
275 widely used for various hydrological and/or environmental application in different regions of
276 the world (Gassman et al., 2014). Furthermore, the capability of SWAT model to be easily
277 linked with calibration, sensitivity analysis and uncertainty analysis tools (e.g., SWAT-CUP)
278 made it more preferable.

279 SWAT model follows a two-level discretization scheme: i) sub-basin creation based on
280 topographic data and ii) Hydrological Response Unit (HRU) creation by further discretizing
281 the sub-basin based on land use and soil type. HRU is a basic computational unit assumed to
282 be homogeneous in hydrologic response. Hydrological processes are first simulated at the HRU
283 level and then routed at the sub-basin level (Neitsch et al., 2009). The SWAT model estimates
284 surface runoff using the modified USDA Soil Conservation Service (SCS) curve number
285 method. In this study, a minimum threshold area of 400 km² were used for determining the
286 number of sub-basins and 5% threshold for the soil, slope, and land use were used for the HRU
287 definition. Accordingly, 13 sub basins and 350 HRUs are created for the Arjo gauging station
288 as outlet.



289 2.3.3. SWAT model calibration and validation

290 Hydrologic modelling performance evaluation technique is commonly performed by
291 either calibrating the hydrologic model with gauge rainfall data and then validating with SREs,
292 (i.e., static parameters) or calibrating and validating the model independently with each rainfall
293 products (i.e., dynamic parameters) and then compare accuracies of the streamflows predicted
294 using the capacity of the rainfall products. The latter is preferred for watersheds such as the
295 DRB where gauging stations are sparse and unevenly distributed. Moreover, studies have
296 reported that independently calibrating the hydrologic model with SREs and gauge data
297 improves performance of the hydrological model (Zeweldi et al., 2011; Vernimmen et al.,
298 2012; Lakew et al., 2017).

299 Calibration, validation and sensitivity analysis of SWAT was done using the SWAT-
300 CUP software. The Sequential uncertainty fitting (SUFI-2) implemented in SWAT-CUP was
301 used in this study (Abbaspour et al., 2007). SUFI-2 provides more reasonable and balanced
302 predictions than the generalized likelihood uncertainty estimation (GLUE) and the parameter
303 solution (ParaSol) methods (Zhou et al., 2014; Wu and Chen et al., 2019) offered by the tool.
304 It also estimates parameter uncertainty attributed to input data, and model parameter and
305 structure as total uncertainty (Abbaspour, 2015). The total uncertainty in the model prediction
306 is commonly measured by *P*-factor and *R*-factor. *P*-factor represents the percentage of observed
307 data enveloped by the 95 percent prediction uncertainty (95PPU) simulated by the model. The
308 *R*-factor represents the ratio of the average width of the 95PPU band to the standard deviation
309 of observed data. For realistic model prediction, *P*-factor ≥ 0.7 and *R*-factor ≤ 1.5 is desirable
310 (Abbaspour et al., 2007, Arnold et al., 2012).

311 The first steps in SWAT model calibration and validation process is determining the
312 most sensitive parameters for a given watershed. For this study, 19 parameters were identified
313 based on the recommendations of previous studies (Roth et al., 2018; Lemann et al., 2019).
314 Global sensitivity analysis was performed on the 19 parameters from which 11 parameters were
315 found sensitive for the DRB, and were used for calibration, verification, and uncertainty
316 analysis. The hydrologic simulations were performed for the 2001 to 2014 period. Two years
317 of spin-up (warm-up) period (i.e., 2001 and 2002), and 6 years of calibration period (2003 to
318 2008), and 6 years of verification periods (2009 to 2014) were used. Graphical and statistical
319 measures were used to evaluate prediction capability of the rainfall datasets. Accordingly, the

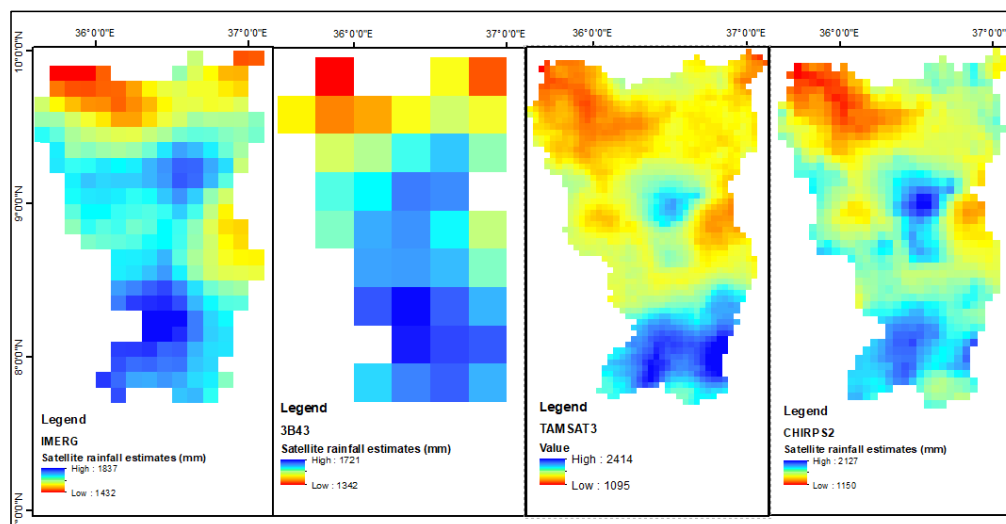


320 performance of model forced by each rainfall datasets was tested using the most widely used
321 statistical indices (i.e., R^2 , NSE and $PBIAS$), in addition to the P -factor and R -factor.

322 3. Results

323 3.1. Statistical evaluation

324 Figure 2 compares mean annual spatial rainfall distributions of the DRB. Average
325 annual rainfall of the study area for the 2001 to 2014 period was 1682.09 mm/year (1150 to
326 2127 mm/year), 1698.59 mm/year (1432 to 1837 mm/year), 1699.06 mm/year (1092 to 2414
327 mm/year) and 1680.28 mm/year (1342 to 1721 mm/year) according to the CHIRPS2, IMERG6,
328 TAMSAT3 and 3B43 products, respectively. For reference, mean annual rainfall for the DRB
329 is 1650 mm/year based on the rain gauge data, which is within 1.8% to 3% of the estimates
330 provided by the products. However, total annual rainfall range estimates were substantially
331 different among the products. The decreasing rainfall trend from the southern (highlands) to
332 the northern (lowlands) part of the basin were captured by all products. In particular,
333 TAMSAT3 and CHIRPS2 captured the rainfall variability in better detail, perhaps due to their
334 high spatial resolution. On the other hand, resolution of the 3B43 rainfall product seems too
335 course to satisfactorily represent spatial variability of rainfall in the basin.



336
337 Figure 2. Spatial mean annual rainfall distribution of the four SREs for DRB (2001 to 2014)

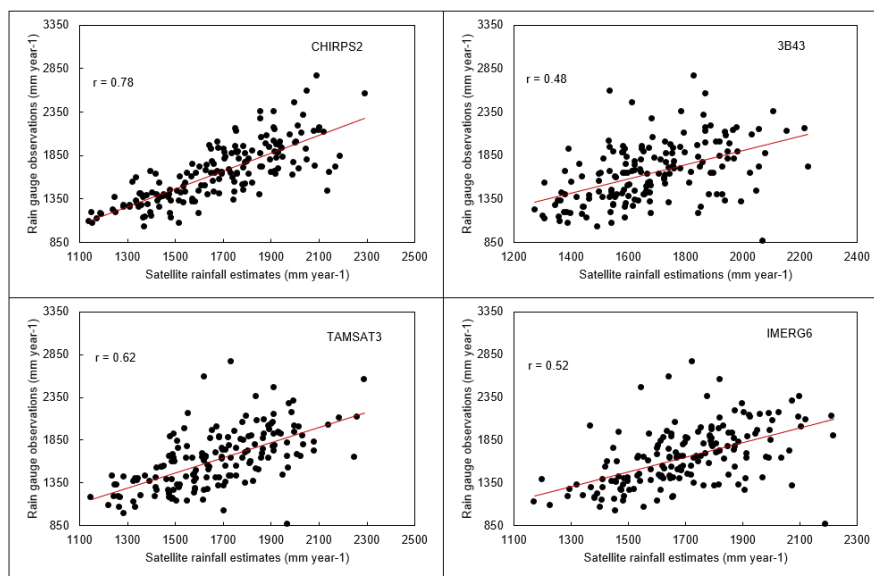
338 Figures 3 to 5 show results of numerical statistical evaluation indices calculated from
339 rainfall from the rain gauges and from the SREs products. More specifically, Figures 3 and 4



340 show correlation coefficients for the annual and monthly timescales, respectively. The results
 341 show that all four SREs products produced rainfall that correlate better to the ground based
 342 rainfall observations at monthly timescale than at annual time scales. The values of statistical
 343 evaluation indices for all products are summarized in Table 3. The results show that the
 344 CHIRPS2 performed better for the DRB with relatively higher r and E , and lower $BIAS$, ME
 345 and $RMSE$ for annual and monthly timescales, respectively.

346 Table 3. Statistical evaluation indices of all SREs.

SREs	R		$BIAS$		ME		$RMSE$ (mm)		E	
	Annual	Monthly	Annual	Monthly	Annual	Monthly	Annual	Monthly	Annual	Monthly
CHIRPS2	0.78	0.92	1.01	1.01	25.94	2.70	214.36	50.48	0.51	0.84
3B43	0.48	0.87	1.02	1.02	30.58	2.55	306.34	62.05	0.76	0.76
IMERG6	0.52	0.90	1.03	1.03	48.87	4.07	299.55	56.95	0.39	0.80
TAMSAT3	0.62	0.89	1.03	1.03	51.46	2.67	274.00	61.28	0.77	0.77

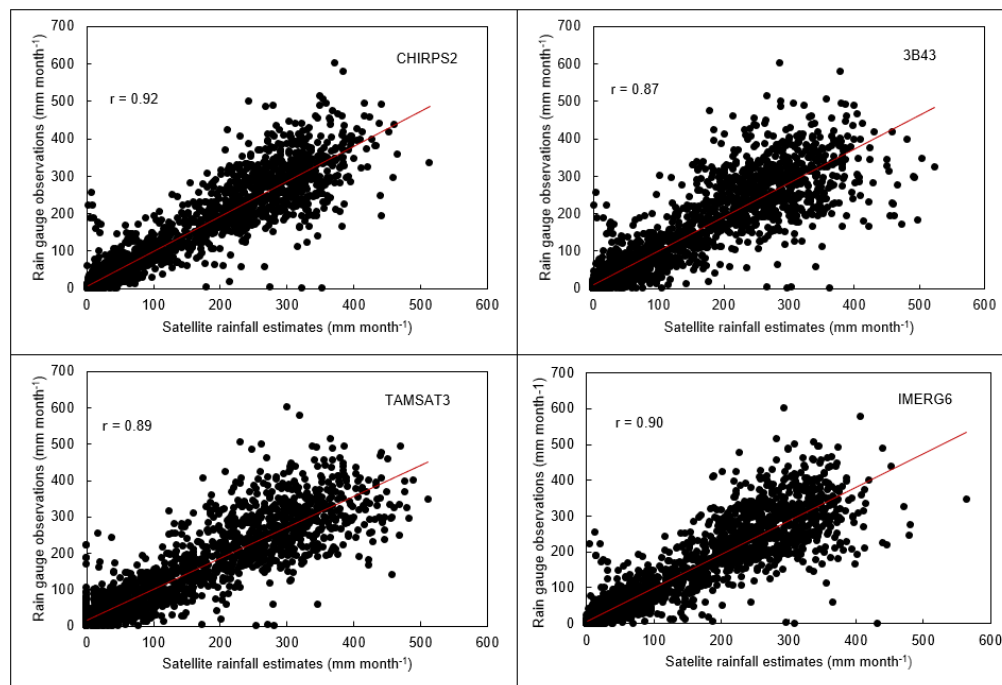


347
 348 Figure 3. Correlation coefficient of the four SREs at annual timescale over DRB.

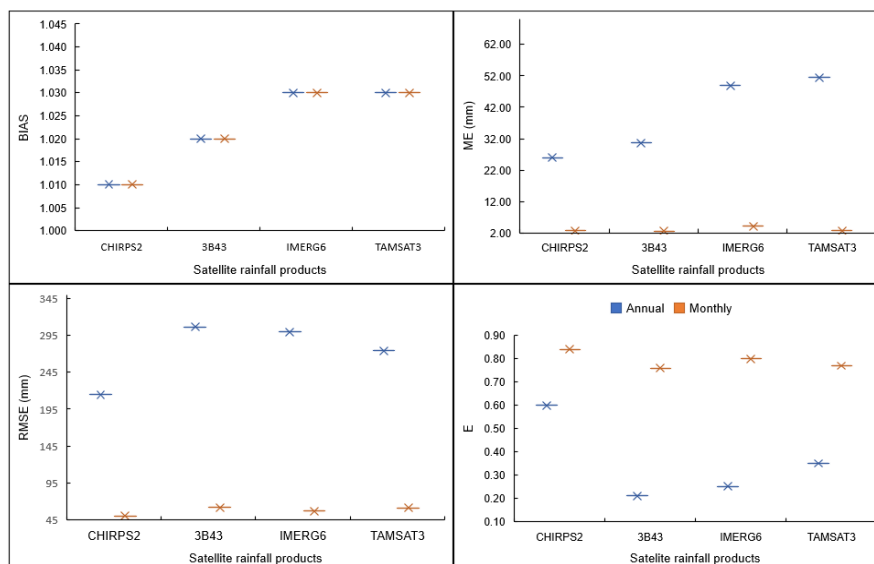
349 Figures 3 to 5 and Table 3 show that generally, CHIRPS2 performed better than the
 350 other three products for the DRB. Correlation coefficients for both monthly and annual
 351 timescales as well as all the indices presented in Figure 5 favor CHIRPS2 indicating its superior
 352 performance. Relative performance of the other three SREs is inconsistent as it varies with the
 353 goodness-of-fit criteria. The 3B43 product, for example, performed worse based on Figure 3



354 and 4 (i.e., correlation coefficients for annual and monthly timescales) and *RMSE* and *E* (Figure
 355 5), but performed better than the other two SREs based on *BIAS* and *ME*.



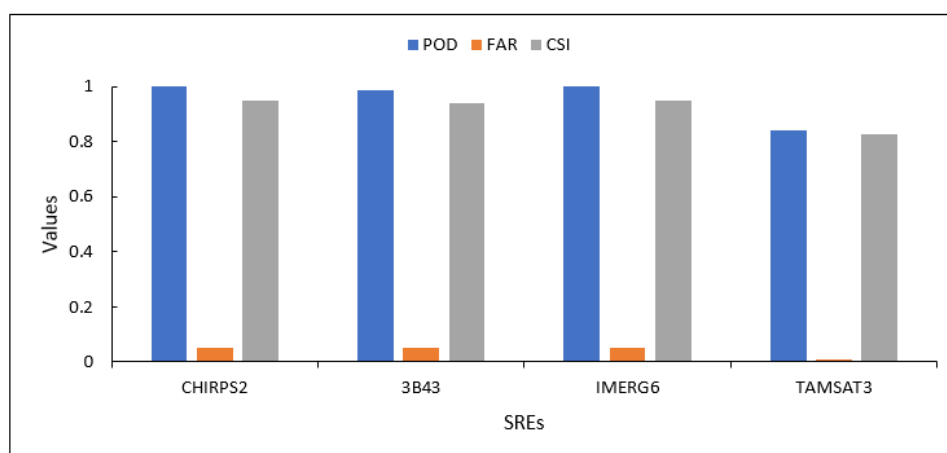
356
 357 Figure 4. Monthly correlation coefficient of the four SREs for the DRB.



358
 359 Figure 5. Statistical indices of the four SREs for DRB at annual and monthly time scales

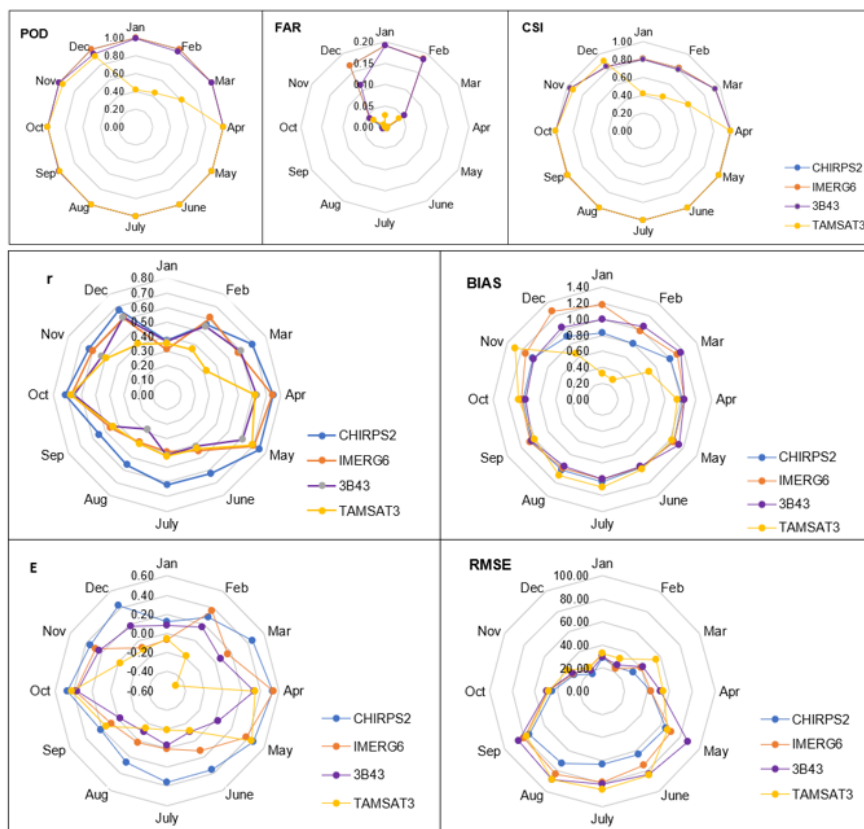


360 Categorical analysis result (Figure 6) shows that all the SREs considered in this study
361 have high rainfall detection capability for the DRB. The *POD* and *CSI* values are close to 1 for
362 all products, and *FAR* values are near 0, which shows that the SREs products have good rainfall
363 event detection and estimation skills. However, TAMSAT3 exhibited relatively less rainfall
364 detection skill, which could be attributed to the sensitivity of TAMSAT3 to topographic effects.



365
366 Figure 6. Categorical indices of the four SREs for the DRB.

367 Figure 7 shows seasonal SREs performance evaluation results. The Figure generally
368 shows that performance of the SREs varied from season to season and among the rainfall
369 products. For example, CHIRPS2 is superior in detecting and estimating rainfall events for the
370 DRB for all months (seasons). The rainfall detection and estimating capability of CHIRPS2 is
371 better for rainy season compared to the dry season. Likewise, the rainfall detection capability
372 of TAMSAT3 is stronger for the rainy season (May to November) but weaker for the dry season
373 (December to April). Compared to the other SREs products, TAMSAT3 generally poorly
374 correlated for all months (seasons), and its *BIAS* was the highest for rainy season but the lowest
375 for the dry season.



376

377 Figure 7. Seasonal statistical evaluation result comparison of each SREs for the DRB.

378 3.2. Hydrological modelling performance evaluation

379 The centroid of each sub basins were used as gauging locations, and used for extracting
380 rainfall for all the SREs rainfall datasets. Thus, each sub basins are represented by a separate
381 and dense gauges unlike that of the measured rainfall representation. The performance of the
382 rainfall products were evaluated using SWAT-CUP at monthly time steps.

383 Table 4 shows details of the calibrated parameters including their ranges, best fit values,
384 sensitivity ranks when different rainfall datasets are used as inputs for the DRB. The table
385 shows that ranges and the best fit values vary from rainfall data source to another. This indicates
386 that accurate characterization of rainfall variability is very critical for reliable hydrological
387 predictions. This finding is consistent with studies that reported that different precipitation
388 datasets influence model performance, parameter estimation and uncertainty in streamflow

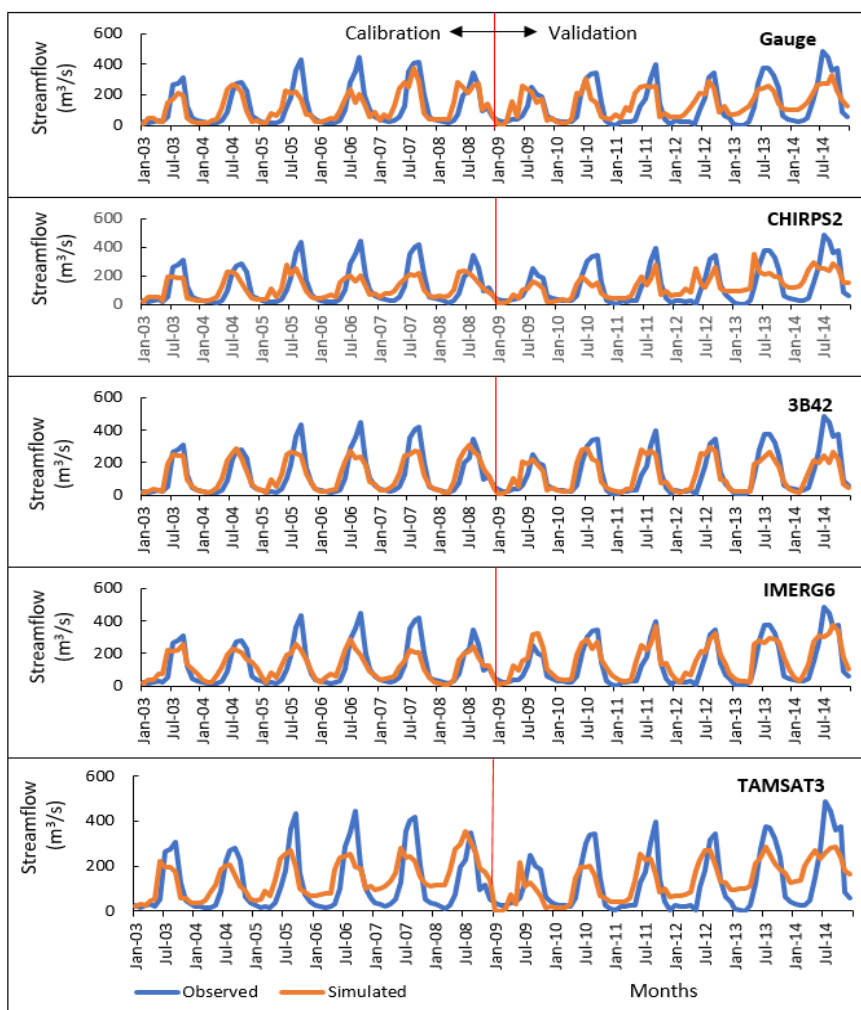


389 predictions (Sirisena et al., 2018; Goshime et al., 2019). Relative sensitivity of the parameters
 390 also varied between the rainfall datasets. In general, *GWQMN.gw*, *ALPHA_BF.gw*,
 391 *GW_DELAY.gw*, *RCHRG_DP.gw*, and *CN2.mgt* are top five sensitive parameters. This seems
 392 indicate that groundwater processes dominate streamflow in the DRB. This could be attributed
 393 to the dominantly deep and permeable soil, vegetated land surface and dominant tertiary
 394 basaltic rocks in the DRB (Conway, 2000; Kabite and Gessesse, 2018).

395 Table 4. Initial parameter ranges, fit values, and sensitivity ranks for rainfall data sources.

Parameters	Initial values	Gauge		CHIRPS2		IMERG6		3B42		TAMSAT3	
		Fit value	Rank								
<i>v_GWQMN.gw</i>	0 to 5000	4936.02	1	201.64	3	3379.76	3	4784.74	1	-0.15	1
<i>v_ALPHA_BF.gw</i>	0 to 1	0.00	2	0.45	4	0.04	4	0.00	2	0.00	2
<i>v_GW_DELAY.gw</i>	0 to 500	339.10	3	29.02	5	34.76	6	391.13	4	318.08	3
<i>v_RCHRG_DP.gw</i>	0 to 1	0.02	4	0.44	7	0.04	5	0.30	3	0.04	4
<i>r_CN2.mgt</i>	-0.25 to 0	310.12	5	-0.25	11	-0.17	10	-0.13	5	-0.15	5
<i>r_SOL_K.sol</i>	0 to 2000	260.96	6	1086.63	9	391.90	11	286.12	6	447.41	6
<i>v_CH_N2.rte</i>	-0.01 to 0.3	0.74	7	0.02	1	0.05	1	0.29	8	0.61	7
<i>CH_K2.rte</i>	-0.01 to 500	310.12	8	354.51	2	426.08	2	256.15	7	298.36	8
<i>v_GW_REVAP.gw</i>	0.02 to 0.2	0.40	9	0.15	8	0.20	8	0.26	9	0.33	10
<i>r_SOL_AWC.sol</i>	-0.5 to 0.5	-0.01	10	-0.49	6	-0.19	7	-0.85	10	-0.59	9
<i>v_REVAPMN.gw</i>	0 to 500	170.26	11	14.52	10	381.84	9	142.11	11	176.48	11

396 Figure 8 compares the observed and the predicted streamflows for the calibration (2003
 397 to 2008) and verification (2009 to 2014) periods for all five rainfall datasets. Goodness of the
 398 streamflow predictions is also summarized in Table 5. The result shows that streamflow is
 399 overestimated for all rainfall products, including the gauge rainfall. This could be due to the
 400 uncertainty of SREs for the extreme rainfall events at daily scale (Jiang et al., 2017). The
 401 overestimated streamflows could also be attributed to overestimation of rainfalls by the SREs
 402 as described in the previous sections. Generally, the indices provided in Table 4 indicate that
 403 the streamflow predictions are satisfactory (Moriassi et al., 2017) for CHIRPS2, IMERG6, and
 404 the gauged rainfall but not for TAMSAT3 and 3B42.



405

406 Figure 8. Graphical calibration and validation of streamflow at monthly scale.

407 Table 5. Calibration and validation results for the different rainfall products.

Rainfall products	Calibration					Validation				
	<i>NSE</i>	<i>R</i> ²	<i>PBIAS</i>	<i>P</i> -factor	<i>R</i> -factor	<i>NSE</i>	<i>R</i> ²	<i>PBIAS</i>	<i>P</i> -factor	<i>R</i> -factor
Gauge	0.55	0.54	2.8	0.43	0.55	0.54	0.57	-9.3	0.15	0.27
CHIRPS2	0.69	0.7	-2.5	0.72	0.64	0.65	0.66	5.3	0.46	0.58
IMERG6	0.65	0.67	2.2	0.70	0.66	0.73	0.78	-14.5	0.64	0.86
TAMSAT3	0.43	0.46	-16.7	0.31	2.94	0.48	0.48	-4.9	0.46	2.68
3B42	0.48	0.51	8.6	0.65	3.88	0.45	0.46	1.3	0.82	2.96

408



409 **4. Discussion**

410 The statistical SREs evaluation result showed that all the rainfall products captured the
411 spatiotemporal rainfall variability of the DRB except the 3B43. Poor performance of 3B43 in
412 capturing basin's rainfall variability is in agreement with findings of two previous studies done
413 for other basins in Ethiopia [Dinku et al., 2008; Worqlul et al., 2014]. The reason could be
414 attributed to the fact that gauge adjustment for 3B43 product did not use adequate gauge data
415 from Ethiopian highlands due to lack of data [Haile et al., 2013]. However, Gebremicael et al.
416 (2019) reported better performance of 3B43 for the Tekeze-Atibara basin, which is located in
417 the northern mountainous area of Ethiopia.

418 Better correlation of SREs with observed rainfall was observed at monthly than at
419 annual timescales for all products. This is consistent with studies that reported the performance
420 of SREs improved with increased time aggregation that peaks at monthly timescale (Dembélé
421 and Zwart, 2016; Katsanos et al., 2016; Zhao et al., 2017; Ayehu et al., 2018; Li et al., 2018;
422 Guermazi et al., 2019). The weak agreement of SREs with observed data at annual timescale
423 shows that the SREs considered in this study generally did not capture the interannual rainfall
424 variability. In this regards, particularly the 3B43 product failed to capture annual rainfall
425 variability compared to the other three SREs. Overall, all four SREs products overestimated
426 rainfall for the DRB by 10% for CHIRPS2 to 30% for IMERG6 and TAMSAT3 (Figure 5).
427 This finding is consistent with studies that reported overestimation of IMERG6 and 3B43
428 products for the alpine and gorge regions of China (Chen et al., 2019). However, Gebremicael
429 et al. (2019) reported underestimation of rainfall by CHIRPS2 for the Tekeze-Atbara basin,
430 which is a mountainous and arid basin in northern Ethiopia. Ayehu et al. (2018) also reported
431 slight underestimation of rainfall by CHIRPS2 for the upper Blue Nile Basin. The discrepancy
432 between our finding and the previous studies done for the basins in Ethiopia may be due to
433 differences in watershed characteristics.

434 Generally, this study showed that the SREs products considered in this study exhibited
435 satisfactory rainfall detection and estimation capability for the DRB. The products are
436 applicable for flood forecasting applications for the DRB (Toté et al., 2015). CHIRPS2
437 performed better than the other three SREs for annual, seasonal, and monthly timescales in
438 detecting and estimating rainfall for the basin. The superiority of CHIRPS2 was also reported
439 by previous studies for different parts of world (Katsanos et al., 2016; Dembélé and Zwart,
440 2016) including basins in Ethiopia (Bayissa et al., 2017; Ayehu et al., 2018; Dinku et al., 2018;



441 Gebremicael et al., 2019). For example, Dinku et al. (2018) reported better rainfall estimation
442 capability of CHIRPS2 for East Africa compared to African Rainfall Climatology version 2
443 (ARC2) and TAMSAT3 products. Ayehu et al. (2018) reported better performance of
444 CHIRPS2 for the Blue Nile Basin compared to ARC2 and TAMSAT3. Better performance of
445 CHIRPS2 has been attributed to the capability of the algorithm to integrate satellite, gauge and
446 reanalysis products and its high spatial and temporal resolution (Funk et al., 2015). On the
447 contrary, generally, the 3B43 rainfall product performed poorly for the DRB for all timescales.
448 This could be due to its coarse spatial resolution and lack of gauge-adjustment for highlands
449 of Ethiopia (Haile et al., 2013). The IMERG6 showed better rainfall detection and estimation
450 capability for the study area than the 3B43 product, which is consistent with findings of
451 previous studies (Huffman et al., 2015; Zhang et al., 2018; Zhang et al., 2019). Better
452 performance of IMERG6 is attributed to the inclusion of dual and high-frequency channels,
453 which improve light and solid precipitation detection capability (Huffman et al., 2015).

454 Hydrologic simulation performance evaluation result of SREs showed that accurate
455 characterization of rainfall variability is very critical for reliable hydrological predictions. This
456 finding is consistent with studies that reported that different precipitation datasets influence
457 model performance, parameter estimation and uncertainty in streamflow predictions (Sirisena
458 et al., 2018; Goshime et al., 2019). Overestimation of streamflow for all SREs products could
459 be attributed to uncertainty of SREs for extreme rainfall events at daily scale (Zhao et al., 2017).
460 The overestimated streamflows could also be attributed to overestimation of rainfalls by the
461 SREs as described in the previous sections.

462 Overall, this study showed that CHIRPS2 and IMERG6 predicted streamflow better
463 than the gauge rainfall and other two SREs products for the DRB. Superior hydrological
464 performance of SREs products compared to gauge rainfall data were also reported by many
465 other studies (Grusson et al., 2017; Bitew and Gebremichael, 2011; Goshime et al., 2019; Xian
466 et al., 2019; Li et al., 2018; Belete et al., 2020). For example, Bitew and Gebremichael (2011)
467 reported that satellite-based rainfall predicted streamflow better than gauge rainfall for complex
468 high-elevation basin in Ethiopia. Likewise, a bias-corrected CHIRP rainfall dataset resulted in
469 better streamflow prediction than a gauge rainfall dataset for Ziway watershed in Ethiopia
470 (Goshime et al., 2019).

471 The relatively poor performance of gauge rainfall compared to the CHIRPS2 and
472 IMERG6 shows that the existing rainfall gauges do not represent spatiotemporal variability of



473 rainfall in the DRB. The rain gauges are sparse, spatially uneven, and incomplete records for
474 the DRB. As previously mentioned, rain gauge density for the DRB is 0.32 per 1000 km²,
475 which is much lower than the World Meteorological Organization (WMO) recommendation
476 of one gauge per 100-250 km² for mountainous areas of tropical regions such as the DRB
477 (WMO, 1994). Overall, this rainfall products performed satisfactorily in terms of detecting
478 and estimating rainfall study showed that CHIRPS2 and IMERG6 rainfall products
479 performed satisfactorily in terms of detecting and estimating rainfall as well as predicting
480 streamflow for the DRB.

481 **5. Conclusions**

482 Satellite rainfall estimates are alternative rainfall data sources for hydrological and
483 climate studies for data scarce regions like Ethiopia. However, SREs contain uncertainties
484 attributed to errors in measurement, sampling, retrieval algorithm and bias correction
485 processes. Moreover, the accuracy of rainfall estimation algorithm is influenced by topography
486 and climatic conditions of a given area. Therefore, SREs products should be evaluated locally
487 before they are used for any application. In this study, we examined the intrinsic data quality
488 and hydrological simulation performance of CHIRPS2, IMERG6, 3B42/3 and TAMSAT3
489 rainfall datasets for the DRB. The statistical evaluation results generally revealed that all four
490 SREs products showed promising rainfall estimation and detection capability for the DRB.
491 Particularly, all SREs captured the south-north declining rainfall patterns of the study area.
492 This could be due to the fact that all the SREs products were gauge adjusted and that they are
493 the latest versions. However, all the SREs datasets overestimated rainfall for DRB. Correlation
494 coefficients of all SREs were strong for the monthly timescales than for the annual timescales,
495 which shows that all rainfall products failed to capture interannual rainfall variability.

496 The quantitative statistical indices showed that CHIRPS2 performed the best in
497 estimating and detecting rainfall events for the DRB at monthly as well as annual timescales.
498 This is likely due to the fact that CHIRPS2 was created by merging satellite, reanalysis and
499 gauge datasets at high spatial resolution. In the contrary, 3B43 performed poorly for the basin.

500 The hydrological modelling based performance evaluation showed that ranges, best fit
501 values, and relative sensitivities of SWAT's calibration parameters varied with the rainfall
502 datasets. Overall, groundwater flow related parameters such as *GWQMN.gw*, *ALPHA_BF.gw*,



503 *GW_DELAY.gw* and *RCHRG_DP.gw* were found more sensitive for all rainfall products. This
504 showed that subsurface processes dominate hydrologic response of the DRB.

505 The hydrological simulation performance results also showed that all the rainfall
506 products, including the observed rainfall, overestimated streamflow especially the high flows,
507 which could be attributed to the uncertainty of SREs rainfall to predict at shorter timescale
508 (e.g., daily) and event rainfalls. The study showed CHIRPS2 and IMERG6 predicted
509 streamflow for the basin satisfactorily, and even outperformed performance of the gauge
510 rainfall. The relatively poor performance of the gauge rainfalls can be attributed to the fact that
511 the gauges are too sparse to accurately characterize rainfall variability in the basin. Overall,
512 CHIRPS2 and IMERG6 products seem to perform better for the Dhidhessa River basin to detect
513 rainfall events, to estimate rainfall quantity, and to improve streamflow predictions.

514 **Funding:** This research did not receive any specific grant from funding agencies in the public,
515 commercial, or not-for-profit sectors.

516 **Supplementary Materials:** Provided up on request.

517 **Author contributions**

518 Gizachew Kabite: Conceptualization, Data collection, analysis and interpretation, writing-
519 original draft preparation.
520 Misgana K. Muleta and Berhan Gessesse: Writing-review and editing. All authors have read
521 and agreed to the published version of the manuscript:

522 **Conflicts of Interest**

523 The authors declare no conflict of interest.

524 **Acknowledgments**

525 We are grateful to the Ethiopian Space Science and Technology Institute for providing partial
526 financial support for this research. We are also thankful to the developers of CHIRPS2,
527 IMERG6, TAMSAT3 and 3B42 datasets and for providing the data free of charge. The
528 National Meteorological Agency of Ethiopia and the Ethiopian Ministry of Water, Irrigation
529 and Energy are also acknowledged for providing climate and streamflow data, respectively.



530 **References**

- 531 Abbaspour, K.C.: SWAT-CUP 2012: SWAT Calibration and Uncertainty Programs-A
532 User Manual; Swiss Federal Institute of Aquatic Science and Technology: Eawag,
533 Switzerland. 2015.
- 534 Abbaspour, K.C., Yang, J., Maximov, I., Siber, R., Bogner, K., Mieleitner, J., Zobrist, J., and
535 Srinivasan, R.: Modelling hydrology and water quality in the pre-alpine/alpine
536 watershed using SWAT, *J. Hydrol.* 333, 413-430, 2007.
- 537 Abera, W., Brocca, L., and Rigon, R.: Comparative evaluation of different satellite
538 rainfall estimation products and bias correction in the Upper Blue Nile (UBN) basin,
539 *Atmos. Res.* 178-179,471-483, 2016.
- 540 Arnold, J.G., Moriasi,D.N., Gassman, P.W., K.C. Abbaspour, M.J. White, R. Srinivasan, C.
541 Santhi, R.D. Harmel, A. Van Griensven, M.W., and Liew, V.: SWAT: Model use,
542 calibration, and validation, *Trans. ASABE.* 55, 1491-1508, 2012.
- 543 Ayehu, G.T., Tadesse, T., Gessesse, B., and Dinku, T.: Validation of new satellite rainfall
544 products over the Upper Blue Nile Basin, Ethiopia, *Atmos. Meas. Tech.* 11, 1921-1936,
545 2018.
- 546 Bayissa, Y., Tadesse, T., Demisse, G., and Shiferaw, A.: Evaluation of satellite-based
547 rainfall estimates and application to monitor meteorological drought for the Upper Blue
548 Nile Basin, Ethiopia, *Remote Sens.* 9,669, 2017.
- 549 Behrangi, A., Khakbaz, B., Jaw,T. Ch., Kouchak, A. A., Hsu, K. and Sorooshian, S.:
550 Hydrologic evaluation of satellite precipitation products over a mid-size basin, *J.*
551 *Hydrolo.* 397,225-237, 2011.
- 552 Belete, M., Deng, J., Wang, K., Zhou, M., Zhu, E., Shifaw, E., and Bayissa, Y.: Evaluation
553 of satellite rainfall products for modeling water yield over the source region of Blue
554 Nile Basin, *Sci. Total Environ.* 708,134834, 2020.
- 555 Bitew, M.M., and Gebremichael, M.: Evaluation of satellite rainfall products through
556 hydrologic simulation in a fully distributed hydrologic model, *Water Resour. Res.* 47,
557 1-11, 2011.
- 558 Brown, J.E.M.: An analysis of the performance of hybrid infrared and microwave satellite
559 precipitation algorithm over India and adjacent regions. *Remote Sens, Environ.* 101,
560 63-81, 2006.



- 561 Chen, J., Wang, Z., Wu, X., Chen, X., Lai, C., and Zeng, Z., Li, J.: Accuracy evaluation of
562 GPM multi-satellite precipitation products in the hydrological application over alpine
563 and gorge regions with sparse rain gauge network. *Hydrol. Res.* 50, 6, 2019.
- 564 Condom, T., Rau, P. and Espinoza, J. C.: Correction of TRMM 3B43 monthly
565 precipitation data over the mountainous areas of Peru during the period 1998-2007,
566 *Hydrol. Process.* 25, 1924-1933, 2011.
- 567 Conway, D.: The Climate and Hydrology of the Upper Blue Nile River, *The Geogr. J.* 1, 49-
568 62, 2000.
- 569 Dembélé, M., and Zwart, S., J.: Evaluation and comparison of satellite-based rainfall
570 products in Burkina Faso, West Africa, *Int. J. Remote Sens.* 37(17), 3995-4014, 2016.
- 571 de Goncalves, L.G.G., Shuttleworth, W.J., Nijssen, B., Burke, E.J., Marengo, J.A., Chou, S.C.,
572 Houser, P., and Toll, D.L.: Evaluation of model-derived and remotely sensed
573 precipitation products for continental South America, *J. Geoph. Res.* 111: D16113,
574 2006.
- 575 Dinku, T., Chidzambwa, S., Ceccato, P., Connor, S. and Ropelewski, C.: Validation of
576 highresolution satellite rainfall products over complex terrain, *Int. J. Remote Sens.*,
577 29, 4097-4110, 2008.
- 578 Dinku, T., Funk, C., Peterson, P., Maidment, R., Tadesse, T., Gadain, H., and Ceccato, P.:
579 Validation of the CHIRPS satellite rainfall estimates over eastern Africa, *Quar. J.*
580 *Roy. Meteo. Soci.* 144, 292-312, 2018.
- 581 Dinku, T., Ruiz, F., Connor, S.J. and Ceccato, P.: Validation and Intercomparison of
582 Satellite Rainfall Estimates over Colombia, *J. Appl. Meteorol. Climatol.* 49, 1004-
583 1014, 2010.
- 584 Funk, C., Verdin, A., Michaelsen, J., Peterson, P., Pedreros, D. and Husak, G.: A global
585 satellite-assisted precipitation climatology, *Earth Syst. Sci., Data.* 7, 275-287, 2015.
- 586 Gassman, P.W., Sadeghi, A.M., and Srinivasan, R.: Applications of the SWAT model
587 special section: Overview and insights, *J. Environ. Qual.* 43, 1-8, 2014.
- 588 Gebremicael, T.G., Mohamed, Y.A., van der Zaag, P., Gebremedhin, M., Gebremeskel, G.,
589 Yazew, E., and Kifle, M.: Evaluation of multiple satellite rainfall products over the
590 rugged topography of the Tekeze-Atbara basin in Ethiopia, *Int. J. Remote Sen.*
591 40(11), 4326-4345, 2019.
- 592 Gebremichael, M., Bitew, M.M., Hirpa, F.A., and Tesfay, G. N.: Accuracy of satellite
593 rainfall estimates in the Blue Nile Basin: Lowland plain versus highland mountain,
594 *Water Resour. Res.* 50, 8775-8790, 2014.



- 595 Geological Survey of Ethiopia (GSE): Geology of the Nekemte and Gimbi Area. Sheet
596 Number: NC-37-9 and NC-36-12, respectively. Unpublished, 2000.
- 597 Goshime, D.W., Absi, R., and Ledésert, B.: Evaluation and Bias Correction of CHIRP
598 Rainfall Estimate for Rainfall-Runoff Simulation over Lake Ziway Watershed,
599 Ethiopia, *Hydrology*, 6:68, 2019.
- 600 Grusson, Y., Antil, F., Sauvage, S., and Perz, S.: Testing the SWAT Model with Gridded
601 Weather Data of Different Spatial Resolution. *Water*, 9:54, 2017.
- 602 Guermazi, E., Milano, M., and Reynard, E.: Performance evaluation of satellite-based
603 rainfall products on hydrological modelling for a transboundary catchment in northwest
604 Africa, *Theo. App. Clim.* 138, 1695-1713, 2019.
- 605 Habib, E., Haile, A. T., Tian, T., and Joyce, R. J.: Evaluation of the High-Resolution
606 CMORPH Satellite Rainfall Product Using Dense Rain Gauge Observations and Radar-
607 Based Estimates, *J. Hydrmeteo.*, 13 (6), 1784-1798, 2012.
- 608 Haile, A. T., Habib, E., Elsaadani, M., and Rientjes, T.: Intercomparison of satellite
609 rainfall products for representing rainfall diurnal cycle over the Nile basin, *Int. J. Appl.*
610 *Earth Obs.* 21, 230-240, 2013.
- 611 Hu, Q., Yang, D., Li, Z., Mishra, A.K., Wang, Y., and Yang, H.: Multi-scale evaluation of
612 six high-resolution satellite monthly rainfall estimates over a humid region in China
613 with dense rain gauges, *Int. J. Remote Sens.* 35, 1272-1294, 2014.
- 614 Huffman, G. J., Bolvin, D. T., Nelkin, E. J., Wolff, D. B., Adler, R. F., Gu, G., Hong, Y.,
615 Bowman, K. P., and Stocker, E. F.: The TRMM Multisatellite Precipitation
616 Analysis (TMPA): quasiglobal, multiyear, combined-sensor precipitation estimates at
617 fine scales, *J. Hydrometeorol.* 8, 38-55, 2007.
- 618 Huffman, G.J., Bolvin, D.T., Braithwaite, D., Hsu, K., Joyce, R.J., Kidd, C., Nelkin, E.J., and
619 Xie, P.: Algorithm Theoretical Basis Document (ATBD), 2015.
- 620 Huffman, G.J., Bolvin, D.T., Braithwaite, D., Hsu, K., Joyce, R., Xie, P., and Yoo, S.H.:
621 NASA global precipitation measurement (GPM) integrated multi-satellite retrievals
622 for GPM (IMERG). In Algorithm Theoretical Basis Document (ATBD); NASA/GSFC:
623 Greenbelt, MD, USA, 2014.
- 624 Jiang, S., Liu, S., Ren, L., Yong, B., Zhang, L., Wang, M., Lu, Y., and He, Y.: Hydrologic
625 Evaluation of Six High Resolution Satellite Precipitation Products in Capturing
626 Extreme Precipitation and Streamflow over a Medium-Sized Basin in China, *Water*,
627 10, 25, 2017.



- 628 Joyce, R. J., Janowiak, J. E., Arkin, P. A., and Xie, P.: CMORPH: a method that produces
629 global precipitation estimates from passive microwave and infrared data at high spatial
630 and temporal resolution, *J. Hydrometeorol.* 5, 487-503, 2004.
- 631 Kabite, G., and Gessesse, G.: Hydro-geomorphological characterization of Dhidhessa
632 River Basin, Ethiopia, *Int. Soil and Water Cons. Res.* 6, 175-183, 2018.
- 633 Kabite, G., Muleta, M.K., and Gessesse, B.: Spatiotemporal land cover dynamics and
634 drivers for Dhidhessa River Basin (DRB), Ethiopia, *Mod. Earth Sys. Environ.* 6,
635 1089-1103, 2020.
- 636 Katsanos, D., Retalis, A., and Michaelides, S.: Validation of a high-resolution
637 precipitation database (CHIRPS) over Cyprus for a 30-year period, *Atmos.*
638 *Res.* 169, 459-464, 2016.
- 639 Kidd, C., and Huffman, G.: Global precipitation measurement. *Meteorol. Appl.* 18,334-
640 353, 2011.
- 641 Kidd, C., Bauer, P., Turk, J., Huffman, G.J., Joyce, R., Hsu, K.L., and Braithwaite, D.:
642 Intercomparison of high-resolution precipitation products over northwest Europe. *J.*
643 *Hydrometeorol.* 13, 67-83, 2012.
- 644 Kimani, M.W., Hoedjes, J.C.B., and Su, Z.: An assessment of satellite-derived rainfall
645 products relative to ground observations over East Africa, *Remote Sens.* 9(5), 430,
646 2017.
- 647 Lakew, H.B., Moges, S.A., and Asfaw, D.H.: Hydrological Evaluation of Satellite and
648 Reanalysis precipitation products in the Upper Blue Nile Basin: A case study of Gilgal
649 Abbay, *Hydrology*, 4, 39, 2017.
- 650 Lemann, T., Roth, V., Zeleke, G., Subhatu, A., Kassawmar, T., and Hurni, H.: Spatial and
651 Temporal Variability in Hydrological Responses of the Upper Blue Nile basin,
652 Ethiopia, *Water*, 11, 21, 2019.
- 653 Li, D., Christakos, G., Ding, X., and Wu, J.: Adequacy of TRMM satellite rainfall data in
654 driving the SWAT modeling of Tiaoxi catchment (Taihu lake basin, China), *J. Hydr.*
655 556, 1139-1152, 2018.
- 656 Maggioni, V., Meyers, P.C., and Robinson, M.D.: A Review of Merged High-Resolution
657 Satellite Precipitation Product Accuracy during the Tropical Rainfall Measuring
658 Mission (TRMM) Era, *J. Hydrometeorol.* 17, 1101-1117, 2016.
- 659 Maidment, R., Emily, B., and Matt, Y.: TAMSAT Daily Rainfall Estimates (Version 3.0).
660 University of Reading. Dataset. doi.org/10.17864/1947.112, 2017.



- 661 Meng, J., Li, Z., Hao, J., Wang, S. Q.: Suitability of TRMM Satellite Rainfall in Driving
662 Distributed Hydrological Model in the Source Region of Yellow River. *J. Hydrol.*
663 509, 320-332, 2014.
- 664 Moriasi, D. N., Arnold, J. G., Van Liew, M. W., Bingner, R.L., Harmel, R.D., and Veith, T.L.:
665 Model evaluation guidelines for systematic quantification of accuracy in watershed
666 simulations. *Trans. American Socie. Agr. Bio. Eng.* 50(3), 885-900, 2007.
- 667 Neitsch, S.L., Arnold, J.G., Kiniry, J.R., and Williams, J.R.: Soil & Water Assessment
668 Tool-Theoretical Documentation Version 2009. Texas Water Resour. Inst, 2009.
- 669 Nesbitt, S.W., Gochis, D.J., and Lang, T.J.: The diurnal cycle of clouds and precipitation
670 along the Sierra Madre Occidental observed during NAME-2004: Implications for
671 warm season precipitation estimation in complex terrain, *J. Hydrometeoro.* 9, 728-
672 743, 2008.
- 673 Nguyen, T.H., Masih, I., Mohamed, Y.A., and Van Der Zaag, P.: Validating rainfall-
674 runoff modelling using satellite-based and reanalysis precipitation products in the Sre
675 Pok catchment, the Mekong River basin, *Geosciences*, 8(5), 164-184, 2018.
- 676 Oromia Water Works Design and Supervision Enterprise (OWWDSE): Dhidhessa Sub-
677 Basin Soil Survey Report. Dhidhessa-Dabus Integrated Land Use Planning Study
678 Project. Unpublished, 2014.
- 679 Roth, V., Lemann, T., Zeleke, G., Subhatu, A.T., Nigussie, T.K., and Hurni, H.: Effects of
680 climate change on water resources in the upper Blue Nile Basin of Ethiopia, *Heliyon*,
681 4(2018) e00771, 2018.
- 682 Seyyedi, H., Angagnostou, E.N., Beinghley, E., and McCollum, J.: Hydrologic evaluation
683 of satellite and reanalysis precipitation datasets over a mid-latitude basin, *Atm.*
684 *Res.* 164-165, 37-48, 2015.
- 685 Sirisena, T.A.J.G., Maskey, S., Ranasinghe, R., and Babel, M.S.: Effects of different
686 precipitation inputs on streamflow simulation in the Irrawaddy River Basin, Myanmar.
687 *J. Hyd.: Reg. Studies.* 19,265-278, 2018.
- 688 Sorooshian, S., Hsu, K.-L., Gao, X., Gupta, H. V., Imam, B., and Braithwaite, D.: Evaluation
689 of PERSIANN system satellite-based estimates of tropical rainfall, *B. Am. Meteorol.*
690 *Soc.* 81, 2035-2046, 2000.
- 691 Stisen, S., and Sandholt, I.: Evaluation of remote-sensing-based rainfall products through
692 predictive capability in hydrological runoff modeling, *Hydrol. Proce.* 24, 879-
693 891, 2010.



- 694 Su, J., Lü, H., Wang, J., Sadeghi, A., and Zhu, Y.: Evaluating the Applicability of Four
695 Latest Satellite-Gauge Combined Precipitation Estimates for Extreme Precipitation
696 and Streamflow Predictions over the Upper Yellow River Basins in China. *Remote*
697 *Sens.* 9, 1176, 2017.
- 698 Tapiador, F.J., Turk, F.J., Petersen, W., Hou, A.Y., García-Ortega, E., Machado, L.A.T.,
699 Angelis, C.F., Salio, P., Kidd, C., Huffman, G.J., et al., Global precipitation
700 measurement: Methods, datasets and applications. *Atmos. Res.* 104-105, 70-97, 2012.
- 701 Thiemig, V., Rojas, R., Zambrano-Bigiarini, M., and Roo, A. D.: Hydrological evaluation
702 of satellite-based rainfall estimates over the Vota and Baro-Akobo Basin, *J.*
703 *Hydrology.* 499, 324-333, 2013.
- 704 Tong, K., Su, F., Yang, D., and Hao, Z.: Evaluation of satellite precipitation retrievals and
705 their potential utilities in hydrologic modeling over the Tibetan Plateau, *J. Hydrol.*
706 519, 423-437, 2014.
- 707 Toté, C., D. Patricio, H. Boogaard, R. Van der Wijngaart, E. Tarnavsky, and Funk, C.:
708 Evaluation of Satellite Rainfall Estimates for Drought and Flood Monitoring in
709 Mozambique, *Remote Sens.* 7 (2), 1758-1776, 2015.
- 710 Vernimmen, R.R., Hooijer, A., Aldrian, E., and Van Dijk, A.I.: Evaluation and bias
711 correction of satellite rainfall data for drought monitoring in Indonesia, *Hydrol.*
712 *Earth Syst. Sci.*, 16, 133-146, 2012.
- 713 WMO: World Meteorological Organization Guide to Hydrological Practices: Data
714 Acquisition and Processing, Analysis, Forecasting and Other Applications. Geneva:
715 Switzerland, 1994.
- 716 Worqlul, A.W., Maathuis, B., Adem, A.A., Demissie, S.S., Langan, S., and Steenhuis, T.S.:
717 Comparison of rainfall estimations by TRMM3B42, MPEG and CFSR with
718 ground-observed data for the Lake Tana basin in Ethiopia, *Hydrol. Earth Syst. Sci.*
719 18, 4871-4881, 2014.
- 720 Wu, H., and Chen, B.: Evaluating uncertainty estimates in distributed hydrological
721 modeling for the Wenjing River watershed in China by GLUE, SUFI-2, and ParaSol
722 methods, *Ecol. Eng.* 76, 110-121, 2015.
- 723 Xian, L., Wenqi, W., Daming, H., Yungang, L., and Xuan, J.: Hydrological Simulation
724 Using TRMM and CHIRPS Precipitation Estimates in the Lower Lancang-Mekong
725 River Basin. *China Geog. Sci.* 29(1), 13-25, 2019.
- 726 Xie, P., and Arkin, A.: An Inter-comparison of Gauge Observations and Satellite Estimates
727 of Monthly Precipitation, *J. Appl. Meteor.* 34, 1143-1160, 1995.



- 728 Xue, X., Hong, Y., Limaye, A.S., Gourley, J.J., Huffman, G.J., Khan, S.I., and Chen, S.:
729 Statistical and Hydrological Evaluation of TRMM-Based Multi-Satellite Precipitation
730 Analysis over the Wangchu Basin of Bhutan: Are the Latest Satellite Precipitation
731 Products 3B42V7 Ready for Use in Ungauged Basins? *J. Hydrol.* 499, 91-99, 2013.
- 732 Yohannes, O.: Water Resources and Inter-Riparian Relations in the Nile Basin: The
733 Search for an integrative Discourse. 270, 2008.
- 734 Yong, B., Chen, B., Gourley, J.J., Ren, L., Hong, Y., Chen, X., Wang, W., Chen, S., and Gong,
735 L.: Inter-comparison of the Version-6 and Version-7 TMPA precipitation products
736 over high and low latitudes basins with independent gauge networks: is the
737 newer version better in both real-time and post-real-time analysis for water resources
738 and hydrologic ext, *J. Hydrol.* 508, 77-87, 2014.
- 739 Zeweldi, D.A., Gebremichael, M., and Downer, C.W.: On CMORPH rainfall for streamflow
740 simulation in a small, Hortonian watershed. *J. Hydrometeorol.* 12, 456-466, 2011.
- 741 Zhang, C., Chen, X., Shao, H., Chen, S., Liu, T., Chen, C., Ding, Q., and Du, H.: Evaluation
742 and Inter-comparison of High-Resolution Satellite Precipitation Estimates-GPM, TRMM, and
743 CMORPH in the Tianshan Mountain Area. *Remote sens.* 10, 1543, 2018.
- 744 Zhang, Z., Tian, J., Huang, Y., Chen, X., Chen, S., and Duan, Z.: Hydrologic Evaluation of
745 TRMM and GPM IMERG Satellite-Based Precipitation in a Humid Basin of China.
746 *Remote Sens.* 11, 431, 2019.
- 747 Zhao, Y., Xie, Q., Lu, Y., and Hu, B.: Hydrologic Evaluation of TRMM Multisatellite
748 Precipitation Analysis for Nanliu River Basin in Humid Southwestern China. *Scie.*
749 *Reports*, 7, 2470, 2017.
- 750 Zhou, J., Liu, Y., Guo, H., and He, D.: Combining the SWAT model with sequential
751 uncertainty fitting algorithm for streamflow prediction and uncertainty analysis for the
752 Lake Dianchi Basin, China. *Hydrol. Process.* 28, 521-533, 2014.